Biochimica et Biophysica Acta 1862 (2016) 46–55

Contents lists available at ScienceDirect

Biochimica et Biophysica Acta

journal homepage: www.elsevier.com/locate/bbadis

GLI2 cell-specific activity is controlled at the level of transcription and RNA processing: Consequences to cancer metastasis

Helle Sadam [a,b,1], Urmas Liivas [a,1], Anna Kazantseva [a,b], Priit Pruunsild [b], Jekaterina Kazantseva [a], Tõnis Timmusk [b], Toomas Neuman [a], Kaia Palm [a,b,*]

[a] Protobios Llc, Mäealuse 4, Tallinn 12618, Estonia
[b] Department of Gene Technology, Tallinn University of Technology, Akadeemia tee 15, Tallinn 12618, Estonia

ARTICLE INFO

Article history:
Received 12 August 2015
Received in revised form 8 October 2015
Accepted 9 October 2015
Available online 14 October 2015

Keywords:
GLI2
Alternative splicing
RNA processing
Cancer
Invasion

ABSTRACT

High activity of GLI family zinc finger protein 2 (GLI2) promotes tumor progression. Removal of the repressor domain at the N terminus (GLI2ΔN) by recombinant methods converts GLI2 into a powerful transcriptional activator. However, molecular mechanisms leading to the formation of GLI2ΔN activator proteins have not been established. Herein we report for the first time that the functional activities of GLI2 are parted into different protein isoforms by alternative promoter usage, selection of alternative splicing, transcription initiation and termination sites. Functional studies using melanoma cells revealed that transcriptional regulation of GLI2 is TGFbeta-dependent and supports the predominant production of GLI2ΔN and C-terminally truncated GLI2 (GLI2ΔC) isoforms in cells with high migratory and invasive phenotype. Taken together, these results highlight the role of transcription and RNA processing as major processes in the regulation of GLI2 activity with severe impacts in cancer development.

1. Introduction

Glioma-associated oncogene proteins 1, 2, and 3 (GLI1, GLI2, and GLI3) belong to the family of Krüppel-like transcription factors with C2H2-Zn finger DNA-binding domains. GLI proteins are the main effectors of the Sonic Hedgehog (Hh) pathway that is important during embryonic development and in adult [1,2]. All three GLI proteins contribute to tumor progression by stimulating cell cycle progression, inhibiting apoptosis [2–4] and promoting tumor cell invasion and metastasis [5–8].

GLI proteins act as transcription activators and repressors depending on the cellular context. All GLI proteins have C-terminal activation domains, whereas GLI2 and GLI3 additionally possess an N-terminal repressor domain [9–11]. Previous studies have found that transcriptional activity of GLI2/3 proteins is controlled via regulated proteolytic processing generating C-terminally truncated repressors (GLI2ΔC and GLI3ΔC). While Hh signaling is central to the transcriptional activity of GLI proteins, numerous studies suggest regulation of expression and activation of GLI2 by signaling pathways other than Hh [12,13]. Recent studies have established the role of TGFbeta signaling in non-canonical activation of GLI2 in melanoma cells with metastatic phenotype [14,15].

Extensive studies of GLI proteins have lasted over 15 years. However, understanding the formation of GLI2 activator proteins has remained vague. Early studies showed that unlike the mouse Gli2, the human counterpart does not contain an N-terminal repressor domain (GLI2ΔN) and acts as a transcriptional activator with a molecular weight of 133 kDa [16]. The structure of human *GLI2* was revisited with the description of transcripts encoding the 162 kDa canonical GLI2 protein which is structurally similar to the mouse Gli2 with an N-terminal repressor domain [9]. With these findings it became obvious that the removal of the N-terminal repressor domain is indispensable for the full exposure of the activator potential of human GLI2 [9,11,17]. Since then, most of the studies on GLI2 function have used recombinant GLI2ΔN isoforms [18–20]. However, the mechanisms for production of GLI2ΔN protein isoforms have remained unknown. Furthermore, detection of endogenous GLI2 proteins with commercially available antibodies has been challenging as the latter could barely identify the canonical form of GLI2 protein of 168 kDa. Instead, isoforms of GLI2 with a weight of 133 kDa and with an unknown molecular origin were predominantly detected [21–23].

Recently it has been shown that *GLI1* is subjected to alternative splicing that leads to the synthesis of the N-terminally truncated isoforms GLI1ΔN [24] and tGLI1 [25]. Compared to the canonical form of GLI1, these isoforms show tissue-specific patterns of expression and function [24–26]. Previous studies of GLI2 have described that the usage of 5′ exons in *GLI2* mRNAs encoding the repressor domain is different in cancer cells [16,17]. In the current study we describe the identification of four mutually exclusive 5′ non-coding exons of human *GLI2* with

* Corresponding author at: Protobios Llc, Mäealuse 4, Tallinn 12618, Estonia.
E-mail address: kaia@protobios.com (K. Palm).
[1] These two authors contributed equally to the work.

http://dx.doi.org/10.1016/j.bbadis.2015.10.008
0925-4439/

different patterns of inclusion in alternatively spliced transcripts detected in normal versus malignant tissues. Because of this, we have revisited the human *GLI2* gene structure. In addition, we analyzed the expression of *GLI2* mRNAs across normal tissues and in cancer, explored the use of transcription start/termination sites and dissected the activity of different promoters in producing functionally distinct isoforms. Finally, we discovered that migrating cells predominantly expressed transcription activator GLI2ΔN and GLI2ΔC isoforms with molecular weights of 133 kDa and 48 kDa respectively. Furthermore, the production of these isoforms was enhanced by TGFbeta1 signaling. These data strongly argue for the critical role of signal-induced post-transcriptional processing of *GLI2* in executing cell-specific activity and governing tumor progression and invasion.

2. Materials and methods

2.1. Ethics statement

Human tissues for RNA analysis and skin for primary dermal fibroblast isolation were obtained from the North-Estonian Regional Hospital, Tallinn, Estonia, with the approval from the local ethics committee (license no. 2234, date of issue 09.12.2010).

2.2. Cell culture

Human cancer cells (ATCC) and primary dermal fibroblasts were grown in DMEM [27] containing 10% FBS [27], 1 mg/ml penicillin [27] and 0.1 mg/ml streptomycin [27] at 37 °C in 5% CO_2. All studies were performed at least in three independent experiments run in triplicates.

2.3. Gene structure analysis

Genomic sequence of the *GLI2* gene was retrieved from GenBank (accession number NM_005270.4). To analyze exon/intron boundaries of the *GLI2* gene, the sequences of PCR products were compared with genome sequences using The Human Genome Browser tool at UCSC (version GRCh37, http://genome.ucsc.edu/). Newly described sequences of *GLI2* were submitted to GenBank — http://www.ncbi.nlm.nih.gov.

2.4. RNA extraction, RT-PCR and qPCR

Commercial RNA samples extracted from primary colon carcinoma (clinical stages I–IV and tumor grades 1–3, patient age range 25–83 years, BioChain Institute, Inc.), primary breast carcinoma (clinical stages I–IV and tumor grades 1–3, patient age range 25–83 years; BioChain Institute, Inc.) and primary melanoma (clinical information unknown, patient age range 42–83 years; BioChain Institute, Inc.) were used for analysis.

Total RNA from human cells was isolated using TRIzol® Reagent (Invitrogen) and total RNA from human tissues was isolated using RNAWiz (Ambion) as recommended by the manufacturer. One microgram of RNA was reverse transcribed into cDNA using SuperScript III first strand cDNA synthesis kit (Invitrogen) according to the manufacturer's instructions. The resulting cDNAs were used as templates for subsequent RT-PCR and qPCR reactions. RT-PCR was carried out by using HotFire Pol® DNA polymerase (Solis Biodyne), 25–45 amplification cycles and an annealing temperature of 58 °C. Amplification of the housekeeping gene *GAPDH* was performed for 25 cycles using Fire Pol® DNA polymerase (Solis Biodyne) and used as an internal control. The nucleotide sequences of primers are given in Table S1. Resulting PCR products were verified by sequencing using the services of GATC Biotech AG (Germany). qPCR was carried out using LighCycler 480 SYBR Green I Master kit (Roche) system, 45 amplification cycles and an annealing temperature of 60 °C using a LightCycler 480 II (Roche) machine and LightCycler 480 SW 1.5 (Roche) software. Expression of *RPLP0* (ribosomal protein, large p0) mRNA was used as an internal control for normalization of target gene expression. The nucleotide sequences of primers and the sizes of amplicons are given in Table S1. The results were analyzed using the $2^{-\Delta\Delta CT}$ method [28]. Three parallels of a single sample were used to calculate mean and standard deviation values. Statistical values were calculated by using Student's *t*-test (* — $p < 0{,}05$, ** — $p < 0005$, *** — $p < 0001$).

2.5. Rapid amplification of cDNA ends (RACE)

5′-RACE and 3′-RACE amplifications were performed with the 5′- and 3′-RACE Systems for Rapid Amplification of cDNA Ends kit (Invitrogen) according to the manufacturer's instructions. In 5′-RACE, first-strand cDNAs were generated by reverse transcription of total RNA from fetal brain and LoVo cells using primers p14 and p16 specific to exon V or exon XV of *GLI2*, respectively (shown in Table S1). Amplicons were re-amplified using nested *GLI2*-specific primers p15 or p17 (shown in Table S1) and AUAP (Invitrogen). In 3′-RACE, first-strand cDNA was generated by using polyA+ adapter primers (Invitrogen). The cDNA was amplified by PCR using primer p18 specific to exon XII of *GLI2* (shown in Table S1) and AUAP (Invitrogen). All amplification reactions were carried out according to the suggested thermocycler conditions of the RACE protocols (Invitrogen). All nested PCR products were cloned in the pCRII-Topo vector (Invitrogen) and analyzed by sequencing (GATC Biotech AG, Germany).

2.6. Cloning, transfection and promoter luciferase assay

A 586 bp fragment (−541 to +45 bp) of the 5′-region of *GLI2* exon I, 584 bp fragment (−481 to +103 bp) of the 5′-region of exon II, a 714 bp fragment (−442/−584 to +272/+130 bp) of the 5′-region of exon III and 575 bp fragment (−561 to +14 bp) of the 5′-region of exon XI were PCR amplified and subcloned into the luciferase reporter vector pGL3-luc-egfp (mod. Promega Corp.). All constructs were verified by sequencing (GATC Biotech AG) and designated as *GLI2*-prom1-luc (P1), *GLI2*-prom1-luc (P2), *GLI2*-prom1-luc (P3) and *GLI2*-prom6-luc (P4). Reporter plasmids were cotransfected with pGL3-CMV-FFLuc vector into U373, SkMel-28, MDA-MB 231, WM266-4 and A375M cells using the Amaxa Cell line 96-well Nucleofector Kit SE (Lonza) according to the manufacturer's instructions. Control samples were obtained by transfecting the cells with pGL3-luc-egfp vector. Promoter activity was assayed by the Dual-Glo luciferase reporter assay system (Promega Corp.), where the Renilla luciferase activity was used as a control to standardize the transcription efficiency. The data are represented relatively to the pGL3-luc-egfp control vector transfection efficiency. Results represented are the mean values and standard deviations from at least three independent transfections performed in triplicates.

2.7. Ribonuclease protection assay

For construction of plasmids for probe synthesis, DNA fragments specific for the GLI2 exons X to XII and exons XIII to exon XV extension were amplified from cDNA template from the A375M cells using a mix of FirePol (Solis Biodyne) and Pfu (Fermentas) enzymes. PCR products were cloned into StrataClone pSC-A vector (Stratagen) and verified by sequencing. For probe production, the plasmids were linearized with XhoI and antisense RNA was synthesized using Ambion MAXI Script T7/T3 kit according to the manufacturer's instructions using ^{32}P-UTP. RPA was performed as described previously [8,27] using the RPA kit from Ambion and 40 μg of total RNA of A375M and 2.5×10^5 CPM of radiolabeled probe. The protected fragments were separated in 5% acrylamide–urea gel, visualized by autoradiography and quantified with ImageQuant T4 software (Amersham Biosciences). The housekeeping gene *GAPDH* was used as control.

2.8. Western blotting

For protein analysis of isoforms, 30 μg of nuclear protein extracts from A375M cells were prepared by using NE-PER Nuclear and Cytoplasmic Extraction Reagents (Thermo Scientific). For analysis of migrated and non-migrated A375M melanoma cells, 50 μg of whole cell extracts were prepared by using RIPA buffer. The resulting extracts were resolved by 1.5 mm 7% SDS-polyacrylamide gel electrophoresis and transferred onto PVDF membranes (Amersham). The primary antibodies used were: anti-GLI2 (Santa Cruz Biotechnology sc-28674; Santa Cruz Biotechnology sc-20291; R&D Systems AF3635), anti-LaminB1 (Abcam ab16048) and anti-GAPDH (Sigma G8795). The secondary antibodies consisted of HRP-conjugated anti-rabbit, anti-mouse and anti-goat IgGs from Abcam. The ECL-femto kit (Pierce) was used for detection of immunoblotted target proteins. ImageJ ver. 1.47 was used for quantification of Western blot results. Average and standard deviation values were calculated from multiple independent quantifications of a single blot.

2.9. Cell treatments and in vitro invasion/migration assay

Melanoma A375M cells were treated with 10 ng/ml TGF-β1 (Peprotech EC) for 24 h, whereupon RNA was extracted and RT-PCR analysis was performed as described above. Cellular invasion was analyzed using a transwell migration assay (QCM™ 24-Well Colorimetric Cell Migration Assay (Millipore)). For ECM synthesis and the following invasion assay, membranes were coated with 7×10^5 primary dermal fibroblasts. After 24 h growth on the membranes, fibroblasts were lyzed with hypotonic buffer (10 mM Tris; 1 mM EDTA pH 7.4) and removed. The upper chamber was seeded with 200,000 melanoma cells per well. The bottom chamber contained normal medium, including 10% FBS as the chemoattractant, whereas the medium in the upper chamber was without FBS. After 20 h of transwell migration, the membrane was stained with Cell Stain solution (Millipore) according to the manufacturer's instructions. The population of non-migrated cells in the upper chamber was removed and subjected to RNA extraction and RT-PCR analysis or protein extraction and Western blot analysis as described above. For measuring the number of cells migrating towards the chemoattractant, cells on the underside of the membrane were counted using a Nikon Eclipse 80i digital microscope. The insert with the remaining population of cells was placed into the Extraction Buffer (Millipore) and the absorption of the extracted dye was analyzed at OD value 560 nm for determination of viable cell numbers. The cells that migrated across the membrane were used for subsequent RNA extraction and PCR analysis or protein extraction and Western blot analysis as described above. All TGF-β1 treatments and invasion/migration assays were carried out in triplicates.

3. Results

3.1. Use of alternative transcription start and termination sites creates diversity in GLI2 transcripts

Our initial aim was to delineate the role of splicing in regulation of GLI2 activity in different types of cancer. For that we analyzed tissue samples from primary colon carcinoma (clinical stages I–IV and tumor grades 1–3, patient age range 25–83 years), primary breast carcinoma (clinical stages I–IV and tumor grades 1–3, patient age range 25–83 years) and primary melanoma (clinical information unknown, patient age range 42–83 years) by RT-PCR method. Data analysis revealed a range of different transcripts of *GLI2* of various lengths that were more abundant in tumors and fetal tissues as compared to adult normal tissues (Fig. 1A). Number of novel alternative splice variants (ASV) was found that included four novel exons: one located in the 5′ region (splice variants *v30–v38*) and three in the middle of the coding region (splice variants *v11*, *v18*, *v26*, *v27*, *v37*, *v38*) (Fig. 2). These findings justified the need to edit the existing *GLI2* exon/intron structure nomenclature. According to our revision, *GLI2* gene spans at least twenty exons, four of which are in the 5′ non-coding area and sixteen are in the coding region (Fig. 2B).

To identify the correct transcription start and termination sites, 5′ and 3′ rapid amplification of cDNA ends (5′ and 3′ RACE) analyses of human *GLI2* were performed using fetal brain and LoVo colon cancer cell samples. Four alternative transcription start sites (TSSs), one in exon II, two in exon III, and one in exon XI, were identified (Fig. 2B). The TSS in exon I coincided with the one described by Kimura and colleagues [29], whereas we did not detect any TSS upstream of exon IV, although transcripts initiating from exon IV have been described by Dennler [15]. From 3′ RACE analysis data we found a novel internal alternative polyadenylation site downstream of exon XV (*v40–v41*; Fig. 2C). These data indicated that *GLI2* is extensively regulated by transcriptional start and termination site selection.

Consequently, we took a closer look at the expression of transcripts with TSSs in exons I–III and with the alternative termination site in exon XV by using RT-PCR analysis and transcript-specific primers. Complex patterns of *GLI2* splice variant expression with differential profiles across normal tissues and in cancer were observed (Fig. 1B). It was concluded that exons I, II and III are used in a mutually exclusive manner (Fig. 2C; *v21–v38*) with predominant expression of transcripts starting at exon II (Fig. 1B). In general, alternative splicing affected the 5′ exon usage of *GLI2* more in cancer and fetal tissues as compared to adult (Fig. 1B). In contrast, the abundance of *GLI2* mRNAs with the novel 3′ UTRs was high in adult tissues and cancer, but comparatively low in fetal tissues (Fig. 1B).

In conclusion, findings of the complexity of alternative transcription and termination site usage suggested that transcriptional regulation along with RNA processing might be the key processes determining the tissue-specific activities of GLI2.

3.2. Promoter upstream of exon XI is highly active in metastatic melanoma cells

Identification of several novel TSSs of *GLI2* suggested that multiple alternative promoters regulate the transcription of the gene. To examine the relative strengths of *GLI2* promoters, we used a reporter gene assay and analyzed the promoter activity of regions preceding exons I (P1) (TSS described by Kimura et al. [29]), II (P2), III (P3) and XI (P4) of *GLI2* (novel TSSs identified by 5′ RACE analysis) (Fig. 3A) in different cancer cells (glioma U373, breast cancer MDA-MB 231, melanoma WM266-4, SkMel-28 and A375M cells, Fig. 3B). All regions exhibited distinct transcription promoting activities across cells analyzed (Fig. 3B). Specifically, the activity of promoters P2 and P4 preceding exons II and XI, respectively, was remarkably higher in melanoma cells, whereas the activity of promoters P1 and P3, located upstream of exons I and III respectively, was relatively weaker (except for the high activity of promoter P1 in melanoma A375M cells, Fig. 3B). The activity of promoter P4 governs the synthesis of mRNAs that encode the major activator isoforms of GLI2 with no N-terminal repressor domain and a molecular weight of 133 kDa. Thus our data concluded that *GLI2* expression is controlled by at least four alternative promoters. In addition we found that P4 that precedes exon XI and gives rise to GLI2ΔN activator isoforms is highly active in melanoma cells.

The fact that promoter P1 exhibited exceptionally high activity only in melanoma A375M cells provoked us to examine the usage of alternative promoters coupled with internal transcriptional termination in different melanoma cells (Fig. 3C). Indeed, RT-PCR analysis with transcript-specific primers revealed, that transcripts initiated at exon I and terminated at exon XV* were highly expressed in melanoma A375M cells (Fig. 3D), whereas those with exon II were common to all melanomas, and transcripts starting with exons III and IV [15] were not detected in any of the cells analyzed (Fig. 3D). Thus, the transcriptional regulation of *GLI2* yielding GLI2ΔC isoforms with a molecular

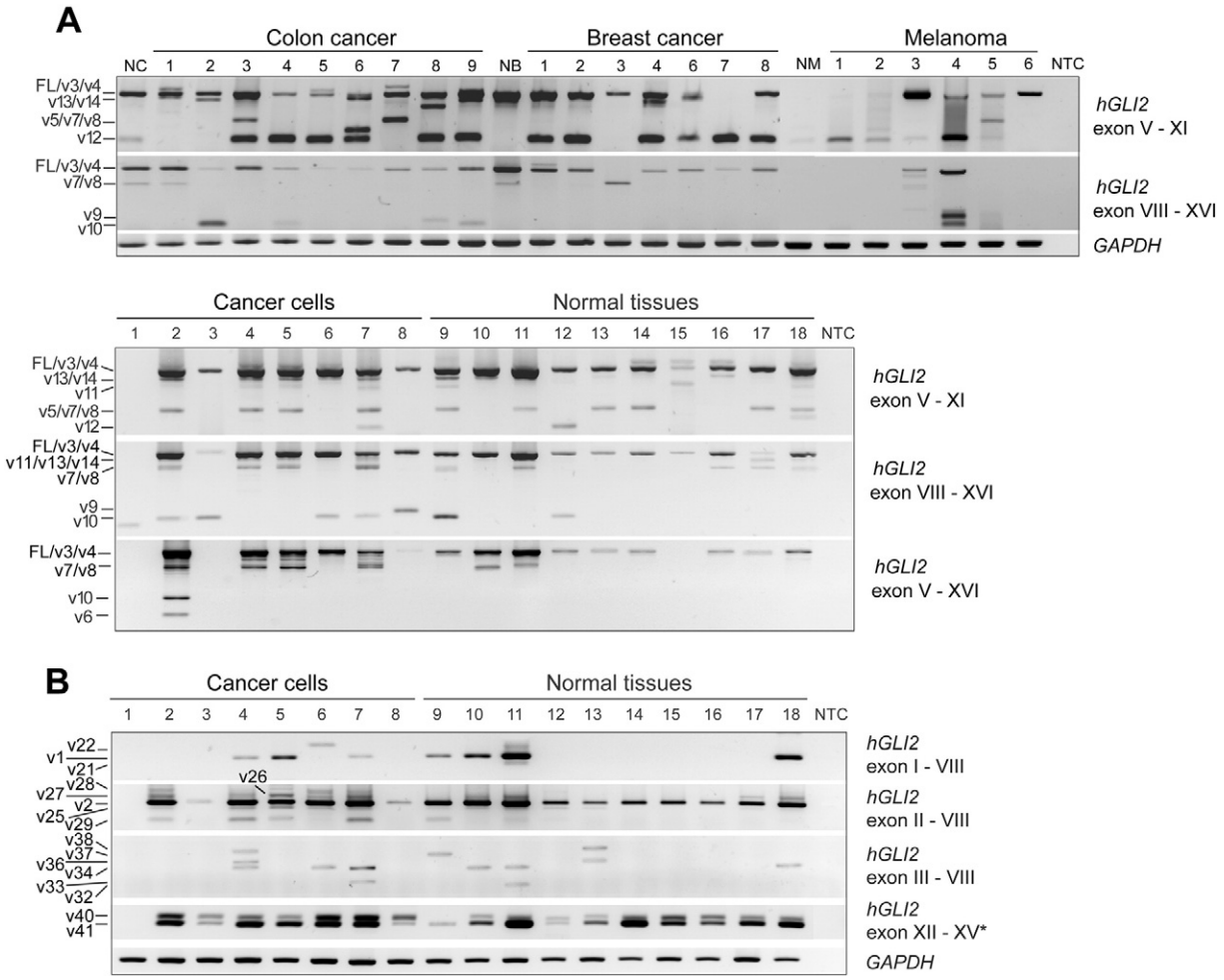

Fig. 1. Expression of alternative splice variants (ASVs) of *GLI2* in different cancer cells and human tissues. A. *GLI2* transcripts are more abundant in cancer cells and fetal tissues than in adult. Cell- and tissue-specific expression of human *GLI2* coding region was analyzed using primer pairs spanning exons V to XVI (see NCBI gene nomenclature on Fig. 2A, see primer sequences and positions in Supplementary Table S1 and Supplementary Fig. S1). For primary cells, we used commercial RNA extracted from colon carcinoma (clinical stages I–IV and tumor grades 1–3, age range 25–83 years, BioChain Institute, Inc.), breast carcinoma (clinical stages I–IV and tumor grades 1–3, age range 25–83 years; BioChain Institute, Inc.) and melanoma (age range 42–83 years; BioChain Institute, Inc.). Cancer cell lines and tissues that were studied in more detail, included: 1. CoLo (colon cancer), 2. LoVo (colon cancer), 3. MCF-7 (breast cancer), 4. Hs578T (breast cancer), 5. SkMel-28 (melanoma), 6. WM266-4 (melanoma), 7. 1321N1 (astrocytoma), 8. U373 (glioblastoma-astrocytoma), 9. fetal brain, 10. fetal colon, 11. fetal skin, 12. adult brain/cerebellum, 13. adult brain/corpus callosum, 14. adult brain/hippocampus, 15. breast, 16. colon, 17. heart, and 18. testis. NC — normal colon, NB — normal breast, NM — normal melanocytes, NTC — negative control, cDNA omitted from PCR reaction. Analysis of *GAPDH* mRNA expression levels was performed to normalize the differences in the amounts of mRNA across samples. FL (full length) indicates the full length *GLI2* mRNA (NM_005270.4), *v_#* indicate corresponding splice variants (see Fig. 2B). B. Expression analysis of *GLI2* mRNAs with alternative 5′ and 3′ UTRs in cancer cells and fetal and adult tissues. Cell- and tissue-specific expression of human *GLI2* 5′ non-coding region was analyzed using primer pairs spanning across exons I and VIII, exons II and VIII and exon IIIs and VIII according to edited nomenclature. To study the expression of transcripts with newly described termination sequences, a primer pair encompassing exons XII to XV extended (XV*) was used (see Table S1 and Fig. S1). 1. CoLo (colon cancer), 2. LoVo (colon cancer), 3. MCF-7 (breast cancer), 4. Hs578T (breast cancer), 5. SkMel-28 (melanoma), 6. WM266-4 (melanoma), 7. 1321N1 (astrocytoma), 8. U373 (glioblastoma-astrocytoma), 9. fetal brain, 10. fetal colon, 11. fetal skin, 12. adult brain/cerebellum, 13. adult brain/corpus callosum, 14. adult brain/hippocampus, 15. breast, 16. colon, 17. heart, and 18. testis, NTC — negative control, cDNA omitted from PCR reaction. Analysis of *GAPDH* mRNA expression was performed to normalize the differences in the amounts of mRNA across samples. *v_#* indicate corresponding splice variants (see Fig. 2C).

weight of 48 kDa is highly effective in A375M cells with the active use of two alternative promoters, P1 and P2.

Altogether, these data suggested that differential regulation of *GLI2* expression is critical for cancer phenotype. Therefore we examined the expression patterns of known melanoma-specific GLI2 target genes in different melanoma cells. As illustrated in Fig. 3E, the patterns of *ZEB1*, *SNAI1*, *CDH1*, *MITF-M*, *TYR* and *TYRP1* expression were highly melanoma cell specific. More precisely, expression of *ZEB1*, that promotes melanoma invasiveness [7] and is a direct target of GLI2 and *SNAI1*, was significantly ($p < 0.05$ or $p < 0.005$) higher in A375M cells as compared with SkMel-28 and WM266-4 cells. In contrast, expression of *CDH1* and *MITF-M*, that are characteristic markers of a less invasive and more proliferative melanoma phenotype [7,8], was relatively lower ($p < 0.05$ or $p < 0.005$) in A375M cells. The expression of MITF-M-associated genes *TYR* and *TYRP1* was also notably weaker in A375M cells as compared with SkMel-28 and WM266-4 cells (Fig. 3E). These data were in good agreement with earlier studies reporting the role of GLI2 in generation of melanoma heterogeneity [6].

In conclusion, these results indicated that increased expression of transcripts encoding GLI2ΔN and GLI2ΔC isoforms correlates with high expression of GLI2 target genes that induce metastatic phenotype of melanoma.

3.3. GLI2ΔN and GLI2ΔC protein isoforms have parted activator and repressor domains

The fact that promoters P1 and P4 exhibited exceptionally high activity in melanoma A375M cells provoked us to further examine the regulation of *GLI2* in those cells. Transcripts encoding GLI2ΔN initiated from P4 preceding exon IX are about 900 nucleotides shorter in their 5′ but otherwise similar to transcripts encoding canonical GLI2. Therefore, we performed ribonuclease protection assay (RPA) to specifically examine the relative levels of expression of transcripts encoding

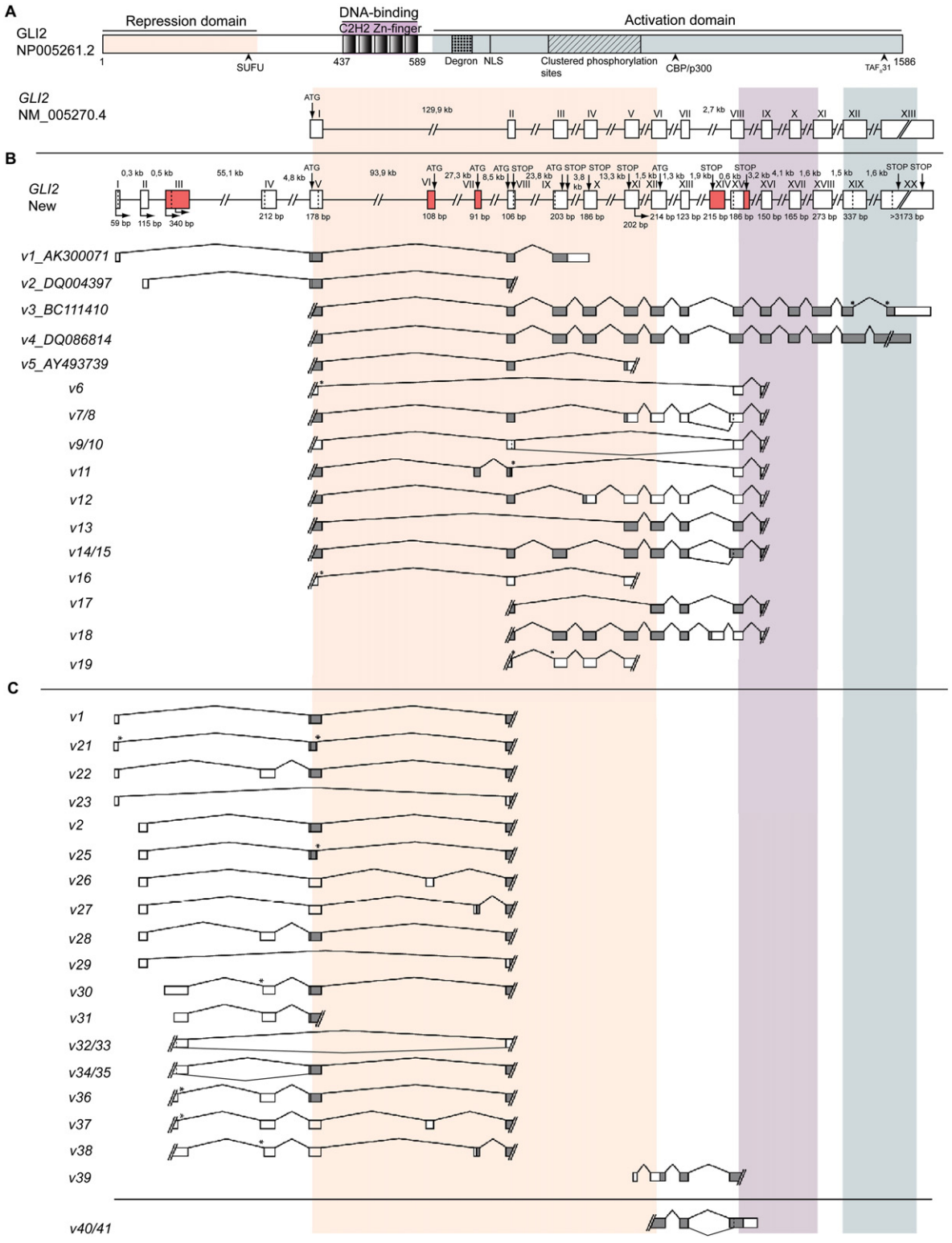

Fig. 2. Genomic organization of *GLI2* locus, alternative splicing patterns and structural domains of GLI2. A. A schematic representation of the human GLI2 protein. Numbers below indicate amino acid positions. Functional domains, nuclear localization signal (NLS) and potential binding sites for regulatory proteins (SUFU, CBP/p300, TAF 31) are shown, diagonally striped box represents the area of phosphorylation sites for PKA, GSK3-beta and CKI, square-filled area shows the degron that directs the starting place of degradation [2,9,11]. Genomic organization of *GLI2* under the scheme of the protein structure is presented according to the NCBI assembly GRCh38.p2 (NG_009030.1). Boxes indicate exons and are drawn to scale, lines indicate introns. The numbers above indicate the sizes of introns. Position of the canonical translation start-site [37] is shown. Roman numbers represent exon numbers. B. Revised genomic organization of *GLI2* and major ASVs. Boxes with Roman numbers above the structure indicate exons and are drawn to scale, lines indicate introns. Red boxes indicate novel exons or exon extensions. The numbers above and below the gene structure indicate the sizes of introns and exons, respectively. Positions of alternative translation start-sites [37] are shown by vertical arrows above the structure. Oriented arrows below indicate the positions of transcription start-sites. Filled boxes indicate the coding region of mRNAs, white boxes represent the non-coding regions. Dashed lines and asterisks (*) indicate alternative donor or acceptor splice-sites. *v1–v5* are previously known splice variants from NCBI assembly Feb. 2009 (GRCh37/hg19). *v6–v19* mRNAs are newly identified splice variants of *GLI2* gene. Major protein domains (Repressor, Zn-finger and Activation) of GLI2 are colored in three different colors and corresponding domains are shown for mRNAs. C. Novel alternative transcripts of GLI2 with newly identified non-coding first exons (*v21–v39*) and exon IX extension (*v40*, *v41*). Boxes with Roman numbers above indicate exons and are drawn to scale, lines indicate introns. Filled boxes indicate the coding region of mRNA, white boxes represent the non-coding region. Asterisks (*) indicate alternative donor or acceptor splice-sites.

GLI2ΔN and GLI2ΔC isoforms. The expression of mRNAs encoding GLI2ΔN was detected by RNA probe 1 spanning exons X to XII (Fig. 4A) generating hybridization products corresponding to the full length *GLI2* (360 bp) and alternative transcripts of *GLI2* with TSSs in exon XI (231 bp) (Fig. 4B). Expression of mRNAs encoding GLI2ΔC was detected with the RNA probe 2 spanning exons XIII to XV extension (marked as XV*) (Fig. 4A) producing full length hybridization products (222 bp) and alternative mRNAs with a termination site in exon XV* (401 bp) (Fig. 4B). Analysis of the housekeeping gene *GAPDH* (530 bp) was used as a control (Fig. 4A–B). These data affirm the endogenous expression of transcripts coding for GLI2ΔN and GLI2ΔC protein isoforms.

In silico analysis of alternatively spliced GLI2 mRNAs predicted that most ORFs start with the canonical ATG located in exon V of *GLI2*, whereas simultaneous exon VI or VII inclusion leads to the formation of isoforms GLI2ΔN$_{-47aa}$ (*v26*, *v37*) and GLI2ΔN$_{-33aa}$ (*v27*, *v38*) containing a deletion in the N-terminal repressor domain (Fig. 2). Alternative ATGs located in exons IX and XII produce protein isoforms GLI2ΔN$_{-125aa}$ (DQ004396) and GLI2ΔN$_{-328aa}$ (AB007295 and AB007296). Isoform GLI2ΔC$_{-1096aa}$ (*v40*, *v41*) with an intact N-terminal repressor domain is, however, the product generated by usage of the alternative polyA site in exon XV* (Fig. 2). Since the effects of partial truncation of the repression and activator domains on GLI2 function are unknown, herein GLI2ΔN$_{-328aa}$ isoforms with no repression domain are referred to as GLI2ΔN, and GLI2ΔC$_{-1096aa}$ isoforms with no activation domain are referred to as GLI2ΔC.

It is well established that most of the commercial anti-GLI2 antibodies recognize the canonical GLI2 protein of 166 kDa and its isoform with a molecular weight of 133 kDa. To our knowledge, none of the studies have ever questioned the nature of the 133 kDa isoform. According to our molecular analysis data this corresponds to the GLI2ΔN isoform (GLI2ΔN$_{-328aa}$). Furthermore, the majority of studies on GLI2 function have used recombinantly produced GLI2ΔN isoforms to analyze the activator function of GLI2 [18–20]. Data from Western blot analysis exploiting three commonly-used anti-GLI2 antibodies revealed the expression of multiple isoforms of GLI2 with molecular weights ranging from ~46 kDa to 168 kDa in a cell-specific manner (Fig. 4C). However, relative to GLI2ΔN (133 kDa) and GLI2ΔC (48 kDa) isoforms, the levels of canonical GLI2 protein of 166 kDa were always detected as low (Fig. 4C). Although GLI2ΔN$_{-47aa}$ and GLI2ΔN$_{-33aa}$ isoforms were not discriminated due to the resolution limitations of Western blot analysis, we detected different C- and N-terminally truncated isoforms of GLI2 with molecular masses ranging from ~55 kDa to ~120 kDa (Fig. 4C). These initial data strongly refer to the need for additional proteomic studies to identify the precise structure of partly truncated isoforms of GLI2. Comparative protein pattern of GLI2 with marked expression of GLI2ΔN (133 kDa) and GLI2ΔC (48 kDa) isoforms was also detected in breast and colon cancer cells (Fig. S2).

These data together with the results from RPA and Western blot analysis further confirmed that cell-specific splicing, alternative initiation and termination of *GLI2* mRNAs results in separating the activator and repressor functions of GLI2 into discrete proteins, GLI2ΔN and GLI2ΔC (Fig. 4D).

3.4. Post-transcriptional processing of GLI2 producing GLI2ΔN and GLI2ΔC isoforms is under the control of TGFbeta1 in invasive melanoma cells

Finally, we examined the relevance of high levels of *GLI2* alternative mRNAs and protein isoforms in metastatic melanoma. Extracellular matrix-coated polycarbonate filter migration assay (Fig. 5A) was used to analyze changes in gene expression upon cell migration. As the transcripts of GLI2ΔN are initiated from P4 preceding exon XI and therefore shortened at their 5′ ends but otherwise similar to transcripts encoding canonical GLI2 protein, we used the semi-quantitative RT-PCR analysis to measure the relative expression of transcripts encompassing exons encoding the N-terminus, the internal region and the C-terminal part of *GLI2* (Fig. 5B). RT-PCR analysis showed that migrating cells expressed high levels of transcripts encoding GLI2ΔC (primers spanning N-terminal exons V to XI and VIII to XI) and GLI2ΔN (primers spanning C-terminal exons XV to XIX) protein isoforms and low levels of full-length *GLI2* mRNAs (primers spanning internal exons VIII to XVI and IX to XVI), as compared with non-migrating cells (Fig. 5B). High expression of novel isoforms of GLI2 was detected by Western blot analysis in migrating cells, namely GLI2ΔN$_{-328aa}$ generated by promoter P4, and GLI2ΔC$_{-1096aa}$ produced due to internal polyadenylation downstream of exon XV, as compared with non-migrating melanoma cells (Fig. 5C). Furthermore, expression of melanoma-specific target genes of GLI2, including *CDH1*, *MITF-M*, *ZEB1* and *SNAI1* was characteristic to migrating cells with a metastatic phenotype (Fig. 5D). Specifically, it was detected that *ZEB1* and *SNAI1* are expressed in an opposite pattern to *CDH1* and *MITF-M* ($p < 0.05$ or $p < 0.005$). To summarize, these data demonstrate that transcription and RNA processing are the key mechanisms driving the expression of GLI2 isoforms with activator function leading to promotion of invasiveness and metastatic character of cancer cells.

Given that *GLI2* is a direct transcriptional target of the TGFbeta1/SMAD pathway [14,15], it was interesting to reveal whether the regulation of alternative splicing of *GLI2* is under the control of TGFbeta1 signaling. TGFbeta1 enhanced the expression of all *GLI2* mRNAs in melanoma A375M cells including those encoding GLI2ΔN and GLI2ΔC (Fig. 5B–C). These data are in harmony with previous findings reporting that autocrine TGFbeta1 activity controls GLI2 expression in melanoma cells [6]. Upon migration both TGFbeta1 treated and untreated melanoma cells predominantly expressed transcripts encoding GLI2ΔN and GLI2ΔC (Fig. 5B). Consistently, expression of GLI2 target genes contributing to migratory phenotype was further enhanced upon TGFbeta1 treatments (Fig. 5D). This supports our previous findings that expression of *GLI2* target genes is strongly affected in cells expressing high levels of GLI2 isoforms with activator functions.

Presented data enable us to conclude that invasive melanoma cells express predominantly GLI2ΔN and GLI2ΔC isoforms under the control of TGFbeta1.

4. Discussion

Analysis of the mechanisms underlying cell-specific activity of GLI2 led us to conclude that: i) the function of GLI2 as a transcriptional activator is controlled at the level of differential promoter usage, alternative splicing and selective initiation and termination of transcription, and ii) isoforms (GLI2ΔN and GLI2ΔC) with transcription activator activity are generated due to the selective and signal-enhanced control of transcription and RNA processing, whereas these isoforms drive the invasive and metastatic potential of melanoma cells.

GLI2 is known for its dual role in the regulation of transcription as it contains an N-terminal repression and a C-terminal activation domain [9]. Despite 15 years of studies, understanding of the molecular mechanisms that govern the formation of activator isoforms of GLI2 has remained vague. Early works by Pan and colleagues [30–32] demonstrated that GLI2 activity is controlled by post-translational proteolytic processing that generates truncated GLI2 isoforms with solely a repressor function. Since proteolysis of GLI2 is a highly inefficient process [32,33], it apparently cannot be the only mechanism for the regulation of GLI2 activity. Most recent studies have found canonical GLI2 to be a weak activator, whereas removal of the N-terminal repressor domain is required for the full exposure of its power as a transcriptional activator [9,17–19]. However, until this study, there has been no molecular understanding of the mechanisms responsible for the generation of GLI2 activator proteins.

Our data show that combinatorial uses of alternative initiation, splicing and termination are the key mechanisms that control the activity of GLI2. We have identified multiple alternatively spliced *GLI2* mRNAs that are expressed at high levels both in normal tissues and in cancer. Because of these findings we were obligated to assign a new exon/intron nomenclature for *GLI2* that provides a better clarity for future studies

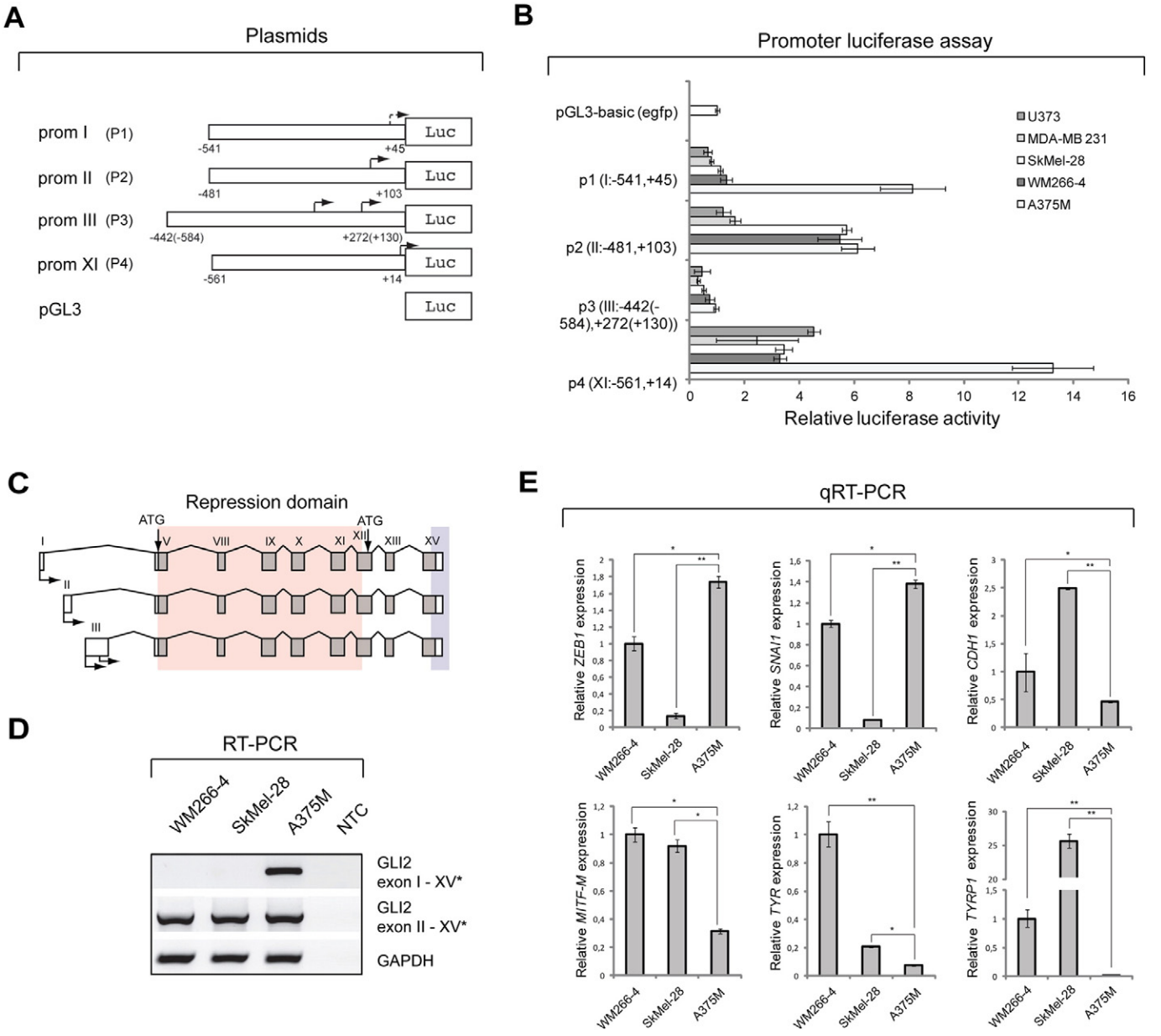

Fig. 3. Promoter upstream of exon XI is highly active in metastatic melanoma cells. A. Schematic representation of *GLI2*-luc reporter constructs used in this study. The locations of the transcription start sites are indicated. B. Multiple promoters of *GLI2* show high activity in A375M melanoma cells. *GLI2* promoter regions were analyzed by luciferase assay in U373, MDA-MB 231, SkMel-28, WM266-4 and A375M cancer cells. The relative activity of the luciferase reporter is normalized to that of pGL3-luc-egfp vector. The activity values were further corrected to the Renilla luciferase activity, which served as the internal reference for the transfection efficiency. Data shown are mean ± SD of three independent experiments. C. A schematic representation of alternative mRNAs encoding GLI2ΔC protein isoforms. Position of the translation start-site [37] is shown by a vertical arrow above the mRNA structure. Oriented arrows below indicate the positions of transcription start-sites. Filled boxes indicate the coding regions of mRNA, white boxes represent the non-coding regions. Protein domains are colored and correspond to domains shown in Fig. 2. D. RT-PCR analysis of alternative transcripts of *GLI2* with exon I revealed melanoma-specific expression of these mRNAs. Expression of *GLI2* transcripts encoding Gli2ΔC was analyzed using primer pairs spanning exons I/II to extended exon XV(*) or XVI (see primer sequences and positions in supplementary Table S1 and supplementary Fig. S1, respectively) in WM266-4, SkMel-28 and A375M melanoma cells. E. Melanoma cells show differential patterns of expression of *GLI2* target genes. Quantitative analysis of expression of *GLI2* target genes (*ZEB1*, *SNAI1*, *CDH1*, *MITF-M*, *TYR*, *TYRP1*, primers in Table S1) was carried out in WM266-4, SkMel-28 and A375M melanoma cells. All results were normalized to expression of *RPLP0*. Data shown are mean ± SD of three independent experiments. Statistical significance is indicated by p-values (Student's t test; * — $p < 0.05$, ** — $p < 0.005$, *** — $p < 0.001$).

(Fig. 2). Cell- and tissue-specific transcription of *GLI2* alternative mRNAs is initiated from several mutually exclusive promoters that precede different 5′ upstream and internal exons. For example, the high activity of promoter P2 preceding exon II is common to most cells, in contrast to cell-specific activity of promoters P1 and P4 preceding exons I and XI. In melanoma A375M cells with metastatic characters, the increased production of GLI2ΔC is driven by promoters upstream of exons I and II (P1 and P2), whereas in less malignant cells only promoter P2 is active.

Furthermore, transcripts initiated from promoter P4 with a TSS in exon XI provide the first evidence of a mechanism for the formation of the 133 kDa GLI2ΔN isoforms with no repressor domain. In 1998, Tanimura and colleagues identified the cDNA encoding GLI2-α that resembles GLI2ΔN in its amino acid sequence [16]. This putative transcript starts at exon IV and is lacking exons VI–XI. We could not detect the *GLI2* transcripts described by Tanimura and colleagues [16] in any of the tissues or cells studied. Given that there are no further data of mRNAs encoding GLI2-α isoforms, these transcripts are extremely rare and

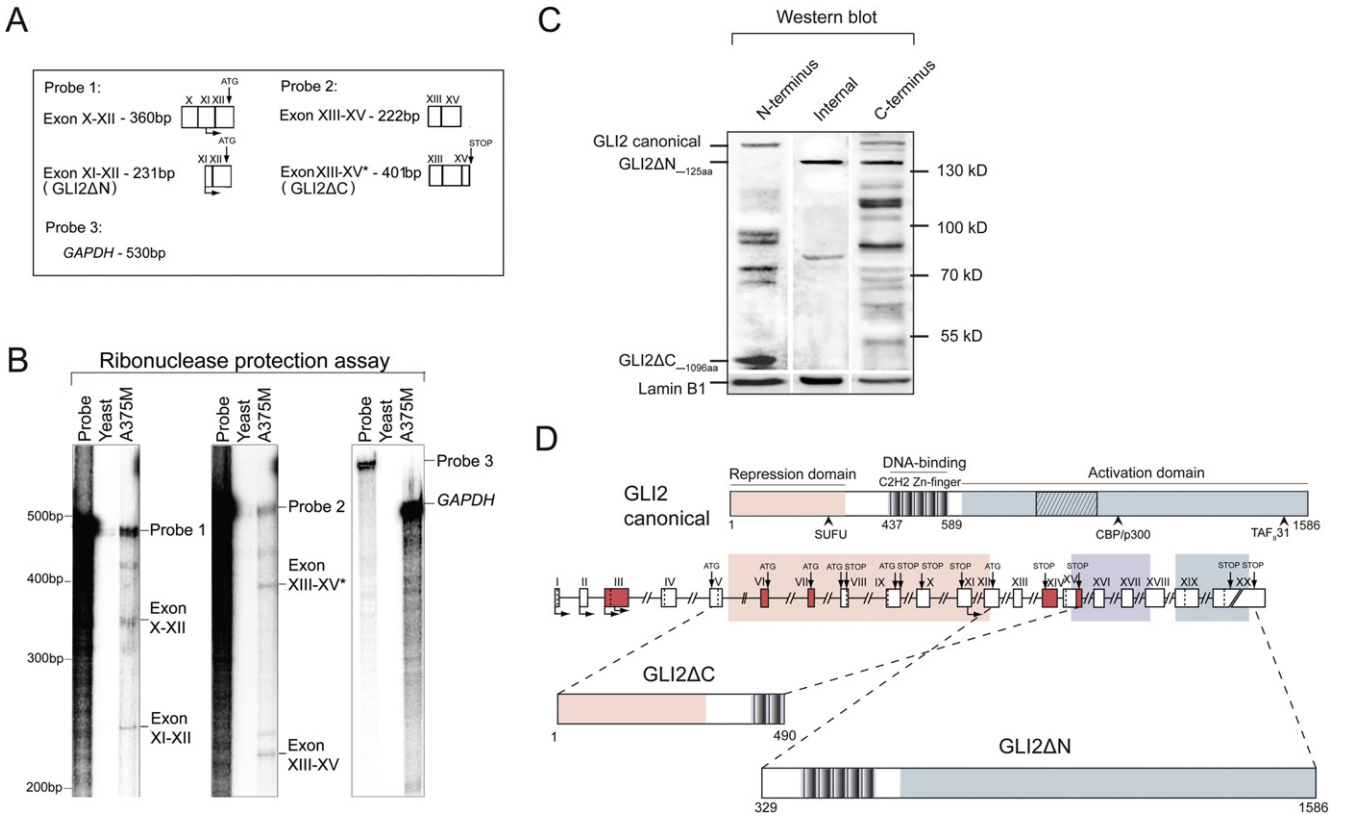

Fig. 4. Melanoma A375M cells express high levels of GLI2 isoforms acting as transcription activators. A. A schematic representation of cDNA probes used for RPA. Probe 1 spanning exons X–XII of *GLI2*; probe 2 spanning exons XIII–XV* of *GLI2*; probe 3 is *GAPDH* specific. B. Expression of transcripts encoding GLI2ΔN and GLI2ΔC proteins was high in melanoma A375M cells as confirmed by RNAse protection assay. Exon structure corresponding to the protected RNA fragments is shown on the right: transcripts with the size 360 bp and 231 bp are designated as exon X-XII (FL) and exons XI–XIII (alternative transcripts of *GLI2* with TSSs in exon XI), or 222 bp as exons XIII–XV* (alternative mRNAs with a termination sites in exon XV*) and 401 bp as exons XIII–XV (FL). RNase H treated (*Yeast*) and untreated yeast RNA (*Probe*) were used as RPA assay controls. C. Melanoma A375M cells express different isoforms of GLI2, whereas predominantly GLI2ΔC and GLI2ΔN as evidenced by Western blotting analysis. For analysis, the following primary antibodies were used: Santa Cruz Biotechnology sc-20291 anti-GLI2 (epitope in the internal region of GLI2), Santa Cruz Biotechnology sc-20291 anti-GLI2 (epitope in the C-terminus of GLI2), and R&D Systems AF3635 anti-GLI2 (epitope in N-terminus of GLI2). Position of the protein molecular weight marker (in kDa) is indicated on the right. Expression of Lamin B1 was analyzed for normalizing purposes. D. GLI2ΔC and GLI2ΔN are the predominant activator forms of GLI2 protein isoforms in cells. Schematic representation of the relatedness of GLI2 protein isoforms to the corresponding genomic regions. Numbers below the structure of the canonical protein indicate amino acid positions. Functional domains and potential binding sites for regulatory proteins (SUFU, CBP/p300, $TAF_{II}31$) are shown, diagonal lines represent the area of PKA, GSK3-beta and CKI phosphorylation sites [2,9,11]. Boxes indicate exons and are drawn to scale, lines indicate introns. Positions of alternative translation start-sites [37] are shown by vertical arrows above the structure. Oriented arrows below indicate the alternative transcription initiation sites, dashed lines indicate translation stop codons. Numbers below the protein structure indicate amino acid positions. Protein domains (Repression, Zn-finger and Activation) are colored (see Fig. 2A). Novel exons characterized by this study are shown in red.

the potential promoter region preceding exon IV is mostly silent. Our study is the first to show that GLI2ΔN isoforms are generated from promoter P4 upstream of exon IX that is widely used in different tissues and cell types. The extensive use of promoter P4 supports promoter-coupled alternative splicing as the major mechanism for generation of GLI2 proteins with an activator domain only (133 kDa GLI2ΔN isoforms). Additionally, we show that the use of the internal polyadenylation site downstream of exon XV results in GLI2ΔC isoforms with no activator domain and disrupted DNA-binding surfaces. Given that GLI2ΔC isoforms are unlikely to bind DNA due to the absence of zinc fingers 3 to 5, they can compete for the interaction with cellular factors targeting the repressor-domain. Furthermore, as isoform GLI2ΔC retains the binding site for Suppressor of fused (SUFU), in most probably counteracts SUFU's activity as a negative regulator of Hh signaling [34,35]. Consistent with this suggestion, earlier overexpression studies with plasmids harboring the repressor domain of *GLI2* (encoded by exons VII–XII) demonstrated that these GLI2ΔC-like proteins acted as transcriptional activators in the presence of canonical GLI2 [9]. These data allow us to conclude that GLI2ΔC functions largely as a transcriptional activator enhancing the activator activity of GLI2. Altogether, our results show for the first time that regulation of *GLI2* transcription supported by alternative splicing allocates the transcriptionally important activator and repressor domains of GLI2 into different isoforms of GLI2ΔN and GLI2ΔC (see Fig. 4D).

We observed that highly metastatic melanoma cells which express a plethora of GLI2 target genes (*ZEB1*, *SNAI1*, *CDH1*, *TYR*, *TYRP1* and *MITF*) supporting melanoma cell invasion have distinct patterns of transcriptional regulation of *GLI2*. We found that migrating cells expressed high levels of transcripts encoding GLI2ΔN and GLI2ΔC, whereas full-length *GLI2* mRNAs and canonical forms of GLI2 were barely detectable. Along with this, the expression of two important metastatic inducers downstream of GLI2, *ZEB1* and *SNAI1* [7], was exclusive to invasive cell population. Based on the results of the current study we propose that signal-induced regulatory mechanisms at the level of transcription and post-transcriptional processing contribute to the cancer-specific activity of GLI2. Recent studies with ectopic expression of recombinant GLI2ΔN have reported induced mesenchymal transition of melanoma cells with enhanced expression of E-cadherin and MITF-M [7] and genomic instability of human epithelial cells [19] are in good correlation with our findings. Our study established that expression of *GLI2* transcripts encoding isoforms with an activator function is under the control of TGFbeta1. Earlier findings have reported both Hh-dependent as well

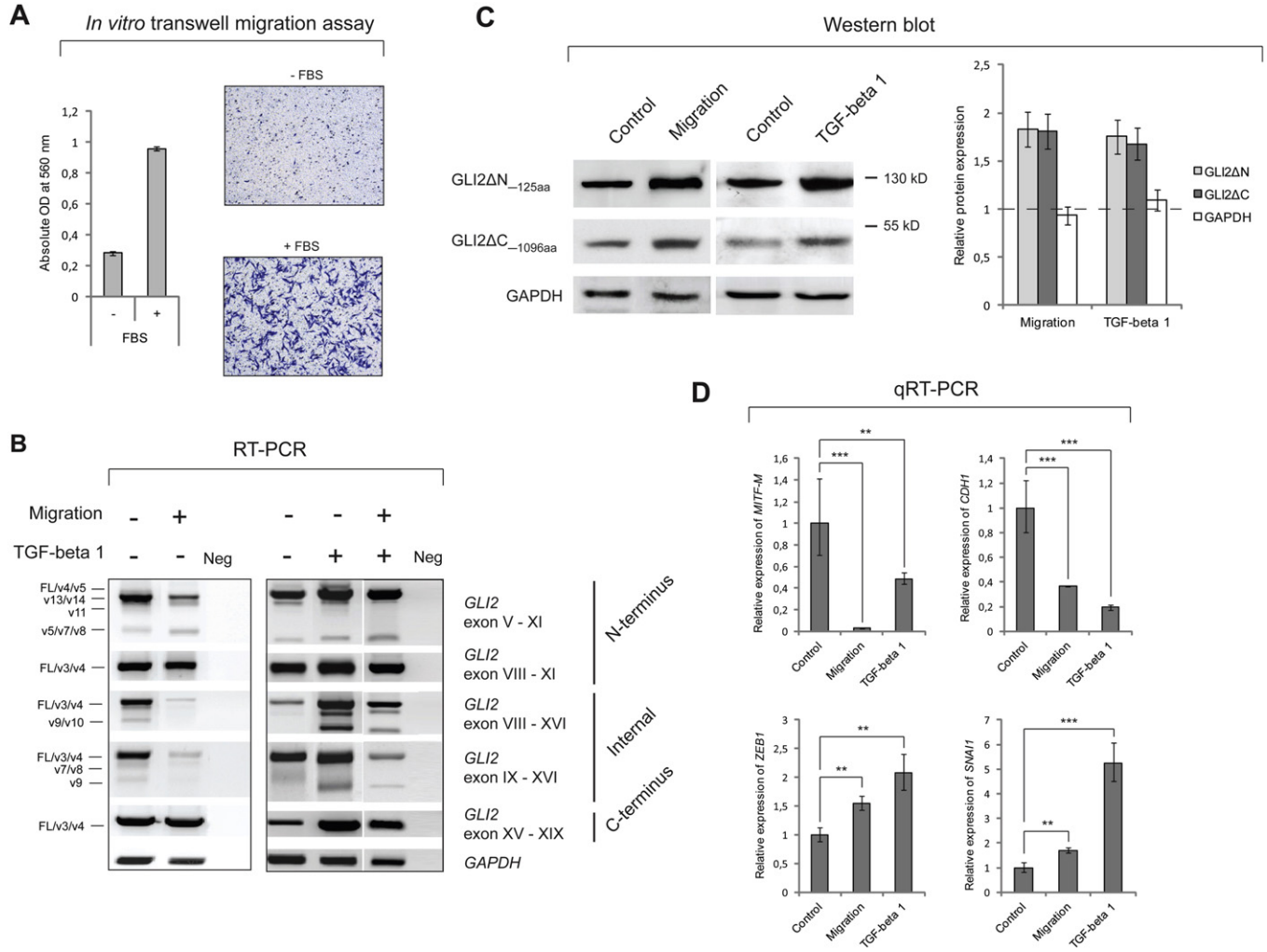

Fig. 5. The effects of migration and TGFβ1 treatment on the expression of GLI2 isoforms and GLI2 target genes in A375M melanoma cells. A. Microscopy pictures of trypan blue stained migrated A375M cells on polycarbonate membranes in the presence (+) or absence (−) FBS as a chemoattractant are shown. FBS is used as an effective chemoattractant for melanoma cell migration stimulation. Graph with the normalized data of OD values of absorption reflecting the number of migrated A375M melanoma cells in response to fetal bovine serum (FBS) is shown on the left. Data are mean ± SD of three independent experiments. B. RT-PCR analysis of *GLI2* expression in migrated (+) and non-migrated (−) and TGFβ1 treated (+) and non-treated (−) A375M cell populations. Analysis of 5′, internal and 3′ regions of *GLI2* transcripts indicate that migrated cells express predominantly transcripts encoding GLI2ΔC and GLI2ΔN upon migration and in response to TGFβ1 treatment. *FL*, *v_#* (*left*) indicate corresponding splice variants (see Fig. 2B). Analyzed exons are provided on the right (see primer sequences and positions in supplementary Table S1 and supplementary Fig. S1, respectively). Neg — negative control, cDNA omitted from PCR reaction. Analysis of *GAPDH* mRNA expression levels (*below*) was performed to normalize the differences in the amount of mRNA across samples. C. Migrated and TGFβ1 treated cells express high levels of GLI2ΔC and GLI2ΔN proteins. Western blotting analysis of GLI2 expression in migrated (+), TGFβ1 treated and non-manipulated (Control) A375M cells. Expression of GAPDH was analyzed for normalizing purposes. Data of quantification of Western blot results is shown on graphs in the right. Results were normalized to the non-migrating/untreated control sample, the relative values of which are represented as dashed line and adjusted to 1. Error bars represent standard deviation. Standard deviations were calculated from multiple independent quantifications of a single blot. Used antibodies: Santa Cruz Biotechnology sc-20291 anti-GLI2, R&D Systems AF3635 anti-GLI2, and Sigma G8795 anti-GAPDH. D. TGFβ1 and cellular migration have similar effects on the expression of GLI2 target genes by supporting motility and invasion. Quantitative expression analysis of GLI2 target genes (*MITF-M, CDH1, ZEB1, SNAI1*, primers in Table S1) in migrated (left graph) or TGFβ1 treated (right graph) A375M cells. All results were normalized to the expression of *RPLP0*. Data shown are mean ± SD of three independent experiments. Dashed line represents the relative levels of gene expression in non-migrated and untreated cells adjusted to 1.

as Hh-independent regulation of GLI activation consequently contributing to tumor progression via acting upon cell cycle, apoptosis and development of metastasis [2–4,20,36]. Regarding TGFbeta1, earlier studies have found this signal-induced mechanism of GLI2 as a key in controlling phenotypic plasticity and invasive behavior of melanoma cells [5,6]. All these data are in good agreement with ours, whereas our findings establish the critical role of RNA processing of *GLI2* that is essential not only its cell-specific activities but also governing cancer (melanoma) progression and invasion.

In conclusion, given that the number of studies on GLI2 function in development and cancer development is increasing, our data emphasize the key role of RNA splicing and processing in controlling the formation of active forms of GLI2 and that targeting of specific alternative splicing events can serve as fine-tuner in important and complex cellular functions of GLI2.

Supplementary data to this article can be found online at http://dx.doi.org/10.1016/j.bbadis.2015.10.008.

Acknowledgments

This study was supported by grants from the Enterprise of Estonia (EU30013), baseline financing from the Estonian Ministry of Education and Research (10.1-8.1/14/509) to Protobios LLC and institutional research funding IUT19-18 from the Estonian Research Council. We thank Maila Rähn and Epp Väli for their technical assistance, Kadri Orro for isolation of dermal fibroblasts, Priit Kogerman for valuable

early discussions and our special thanks goes to Indrek Koppel for help with RPA.

References

[1] C.C. Hui, S. Angers, Gli proteins in development and disease, Annu. Rev. Cell Dev. Biol. 27 (2011) 513–537.
[2] J. Briscoe, P.P. Therond, The mechanisms of Hedgehog signalling and its roles in development and disease, Nat. Rev. Mol. Cell Biol. 14 (2013) 416–429.
[3] A. Ruiz i Altaba, P. Sanchez, N. Dahmane, Gli and hedgehog in cancer: tumours, embryos and stem cells, Nat. Rev. Cancer 2 (2002) 361–372.
[4] A.P. McMahon, P.W. Ingham, C.J. Tabin, Developmental roles and clinical significance of hedgehog signaling, Curr. Top. Dev. Biol. 53 (2003) 1–114.
[5] D. Javelaud, V.I. Alexaki, A. Mauviel, Transforming growth factor-beta in cutaneous melanoma, Pigment Cell Melanoma Res. 21 (2008) 123–132.
[6] V.I. Alexaki, D. Javelaud, L.C. Van Kempen, K.S. Mohammad, S. Dennler, F. Luciani, K.S. Hoek, P. Juarez, J.S. Goydos, P.J. Fournier, C. Sibon, C. Bertolotto, F. Verrecchia, S. Saule, V. Delmas, R. Ballotti, L. Larue, P. Saiag, T.A. Guise, A. Mauviel, GLI2-mediated melanoma invasion and metastasis, J. Natl. Cancer Inst. 102 (2010) 1148–1159.
[7] C.Y. Perrot, C. Gilbert, V. Marsaud, A. Postigo, D. Javelaud, A. Mauviel, GLI2 cooperates with ZEB1 for transcriptional repression of CDH1 expression in human melanoma cells, Pigment Cell Melanoma Res. 26 (2013) 861–873.
[8] M.J. Pierrat, V. Marsaud, A. Mauviel, D. Javelaud, Expression of microphthalmia-associated transcription factor (MITF), which is critical for melanoma progression, is inhibited by both transcription factor GLI2 and transforming growth factor-beta, J. Biol. Chem. 287 (2012) 17996–18004.
[9] E. Roessler, A.N. Ermilov, D.K. Grange, A. Wang, M. Grachtchouk, A.A. Dlugosz, M. Muenke, A previously unidentified amino-terminal domain regulates transcriptional activity of wild-type and disease-associated human GLI2, Hum. Mol. Genet. 14 (2005) 2181–2188.
[10] A. Ruiz i Altaba, Gli proteins encode context-dependent positive and negative functions: implications for development and disease, Development 126 (1999) 3205–3216.
[11] H. Sasaki, Y. Nishizaki, C. Hui, M. Nakafuku, H. Kondoh, Regulation of Gli2 and Gli3 activities by an amino-terminal repression domain: implication of Gli2 and Gli3 as primary mediators of Shh signaling, Development 126 (1999) 3915–3924.
[12] D. Jenkins, Hedgehog signalling: emerging evidence for non-canonical pathways, Cell. Signal. 21 (2009) 1023–1034.
[13] M. Lauth, R. Toftgard, Non-canonical activation of GLI transcription factors: implications for targeted anti-cancer therapy, Cell Cycle 6 (2007) 2458–2463.
[14] S. Dennler, J. Andre, I. Alexaki, A. Li, T. Magnaldo, P. ten Dijke, X.J. Wang, F. Verrecchia, A. Mauviel, Induction of sonic hedgehog mediators by transforming growth factor-beta: Smad3-dependent activation of Gli2 and Gli1 expression in vitro and in vivo, Cancer Res. 67 (2007) 6981–6986.
[15] S. Dennler, J. Andre, F. Verrecchia, A. Mauviel, Cloning of the human GLI2 promoter: transcriptional activation by transforming growth factor-beta via SMAD3/beta-catenin cooperation, J. Biol. Chem. 284 (2009) 31523–31531.
[16] A. Tanimura, S. Dan, M. Yoshida, Cloning of novel isoforms of the human Gli2 oncogene and their activities to enhance tax-dependent transcription of the human T-cell leukemia virus type 1 genome, J. Virol. 72 (1998) 3958–3964.
[17] M. Speek, O. Njunkova, I. Pata, E. Valdre, P. Kogerman, A potential role of alternative splicing in the regulation of the transcriptional activity of human GLI2 in gonadal tissues, BMC Mol. Biol. 7 (2006) 13.
[18] M. Grachtchouk, J. Pero, S.H. Yang, A.N. Ermilov, L.E. Michael, A. Wang, D. Wilbert, R.M. Patel, J. Ferris, J. Diener, M. Allen, S. Lim, L.J. Syu, M. Verhaegen, A.A. Dlugosz, Basal cell carcinomas in mice arise from hair follicle stem cells and multiple epithelial progenitor populations, J. Clin. Invest. 121 (2011) 1768–1781.
[19] E. Pantazi, E. Gemenetzidis, G. Trigiante, G. Warnes, L. Shan, X. Mao, M. Ikram, M.T. Teh, Y.J. Lu, M.P. Philpott, GLI2 induces genomic instability in human keratinocytes by inhibiting apoptosis, Cell Death Dis. 5 (2014), e1028.
[20] D. Javelaud, V.I. Alexaki, M.J. Pierrat, K.S. Hoek, S. Dennler, L. Van Kempen, C. Bertolotto, R. Ballotti, S. Saule, V. Delmas, A. Mauviel, GLI2 and M-MITF transcription factors control exclusive gene expression programs and inversely regulate invasion in human melanoma cells, Pigment Cell Melanoma Res. 24 (2011) 932–943.
[21] Q. Chen, R. Xu, C. Zeng, Q. Lu, D. Huang, C. Shi, W. Zhang, L. Deng, R. Yan, H. Rao, G. Gao, S. Luo, Down-regulation of Gli transcription factor leads to the inhibition of migration and invasion of ovarian cancer cells via integrin beta4-mediated FAK signaling, PLoS One 9 (2014), e88386.
[22] A. Voronova, E. Coyne, A. Al Madhoun, J.V. Fair, N. Bosiljcic, C. St-Louis, G. Li, S. Thurig, V.A. Wallace, N. Wiper-Bergeron, I.S. Skerjanc, Hedgehog signaling regulates MyoD expression and activity, J. Biol. Chem. 288 (2013) 4389–4404.
[23] M.H. Shahi, R. Holt, R.B. Rebhun, Blocking signaling at the level of GLI regulates downstream gene expression and inhibits proliferation of canine osteosarcoma cells, PLoS One 9 (2014), e96593.
[24] T. Shimokawa, U. Tostar, M. Lauth, R. Palaniswamy, M. Kasper, R. Toftgard, P.G. Zaphiropoulos, Novel human glioma-associated oncogene 1 (GLI1) splice variants reveal distinct mechanisms in the terminal transduction of the hedgehog signal, J. Biol. Chem. 283 (2008) 14345–14354.
[25] H.W. Lo, H. Zhu, X. Cao, A. Aldrich, F. Ali-Osman, A novel splice variant of GLI1 that promotes glioblastoma cell migration and invasion, Cancer Res. 69 (2009) 6790–6798.
[26] X. Cao, J. Geradts, M.W. Dewhirst, H.W. Lo, Upregulation of VEGF-a and CD24 gene expression by the tGLI1 transcription factor contributes to the aggressive behavior of breast cancer cells, Oncogene 31 (2012) 104–115.
[27] T. Timmusk, K. Palm, M. Metsis, T. Reintam, V. Paalme, M. Saarma, H. Persson, Multiple promoters direct tissue-specific expression of the rat BDNF gene, Neuron 10 (1993) 475–489.
[28] K.J. Livak, T.D. Schmittgen, Analysis of relative gene expression data using real-time quantitative PCR and the 2(−delta delta C(T)) method, Methods 25 (2001) 402–408.
[29] K. Kimura, A. Wakamatsu, Y. Suzuki, T. Ota, T. Nishikawa, R. Yamashita, J. Yamamoto, M. Sekine, K. Tsuritani, H. Wakaguri, S. Ishii, T. Sugiyama, K. Saito, Y. Isono, R. Irie, N. Kushida, T. Yoneyama, R. Otsuka, K. Kanda, T. Yokoi, H. Kondo, M. Wagatsuma, K. Murakawa, S. Ishida, T. Ishibashi, A. Takahashi-Fujii, T. Tanase, K. Nagai, H. Kikuchi, K. Nakai, T. Isogai, S. Sugano, Diversification of transcriptional modulation: large-scale identification and characterization of putative alternative promoters of human genes, Genome Res. 16 (2006) 55–65.
[30] Z. Li, D. Pan, Y. Li, Effect of TGF-beta on Gli2 expression in HL60 and U937 cell lines, Mol. Med. Rep. 5 (2012) 1245–1250.
[31] Y. Pan, C.B. Bai, A.L. Joyner, B. Wang, Sonic hedgehog signaling regulates Gli2 transcriptional activity by suppressing its processing and degradation, Mol. Cell. Biol. 26 (2006) 3365–3377.
[32] Y. Pan, B. Wang, A novel protein-processing domain in Gli2 and Gli3 differentially blocks complete protein degradation by the proteasome, J. Biol. Chem. 282 (2007) 10846–10852.
[33] Y. Pan, C. Wang, B. Wang, Phosphorylation of Gli2 by protein kinase A is required for Gli2 processing and degradation and the Sonic Hedgehog-regulated mouse development, Dev. Biol. 326 (2009) 177–189.
[34] S.Y. Cheng, S. Yue, Role and regulation of human tumor suppressor SUFU in Hedgehog signaling, Adv. Cancer Res. 101 (2008) 29–43.
[35] D.M. Stone, M. Murone, S. Luoh, W. Ye, M.P. Armanini, A. Gurney, H. Phillips, J. Brush, A. Goddard, F.J. de Sauvage, A. Rosenthal, Characterization of the human suppressor of fused, a negative regulator of the zinc-finger transcription factor Gli, J. Cell Sci. 112 (Pt 23) (1999) 4437–4448.
[36] O. Nolan-Stevaux, J. Lau, M.L. Truitt, G.C. Chu, M. Hebrok, M.E. Fernandez-Zapico, D. Hanahan, GLI1 is regulated through smoothened-independent mechanisms in neoplastic pancreatic ducts and mediates PDAC cell survival and transformation, Genes Dev. 23 (2009) 24–36.
[37] E.W. Humke, K.V. Dorn, L. Milenkovic, M.P. Scott, R. Rohatgi, The output of Hedgehog signaling is controlled by the dynamic association between Suppressor of Fused and the Gli proteins, Genes Dev. 24 (2010) 670–682.